ELSEVIER

Computational Materials Science 28 (2003) 732–742

COMPUTATIONAL MATERIALS SCIENCE

www.elsevier.com/locate/commatsci

Elastoplastic orthotropy at finite strains: multiplicative formulation and numerical implementation

B. Eidel *, F. Gruttmann

Institut für Werkstoffe und Mechanik im Bauwesen (IWMB), TU Darmstadt, Alexanderstr. 7, 64283 Darmstadt, Germany

Abstract

A constitutive model for orthotropic elastoplasticity at finite plastic strains is discussed and basic concepts of its numerical implementation are presented. The essential features are the multiplicative decomposition of the deformation gradient in elastic and inelastic parts, the definition of a convex elastic domain in stress space and a representation of the constitutive equations related to the intermediate configuration. The elastic free energy function and the yield function are formulated in an invariant setting by means of the introduction of structural tensors reflecting the privileged directions of the material. The model accounts for kinematic and isotropic hardening. The associated flow rule is integrated using the so-called exponential map which preserves exactly the plastic incompressibility condition. The constitutive equations are implemented in a brick-type shell element. Representative numerical simulations demonstrate the suitability of the proposed formulations.

PACS: 46.15.−x; 46.35.+z; 46.70.−p
Keywords: Computational solid mechanics; Material modelling; Inelastic constitutive behavior; Large deformations; Anisotropy; Finite element formulation

1. Introduction

Many elastoplastic materials exhibit anisotropic behavior due to their textured or generally orientation dependent structure. The response of anisotropic materials can be described with scalar-valued functions in terms of several tensor variables, usual deformation or stress tensors and additional structural tensors, which reflect the symmetries of the considered material. Based on representation theorems for tensor functions the general forms can be derived and the type and minimal number of the scalar variables entering the constitutive equations can be given. These forms are automatically invariant under coordinate transformations of elements of the material symmetry group. For an introduction to the invariant formulation of anisotropic constitutive equations based on the concept of structural tensors and their representations as isotropic tensor functions see [1–3].

For a state-of-the-art review of the recent progress in the theory and numerics of anisotropic materials at finite strains we refer to the papers published in a special issue of the International Journal of Solids and Structures, vol. 38, 2001,

* Corresponding author. Tel.: +49-6151-16-2439; fax: +49-6151-16-2338.
E-mail address: eidel@iwmb.tu-darmstadt.de (B. Eidel).

0927-0256/$ - see front matter © 2003 Elsevier B.V. All rights reserved.
doi:10.1016/j.commatsci.2003.08.027

EUROMECH Colloquium 394, and the references therein.

The essential features of this paper are summarized as follows:

(i) In our formulation the multiplicative decomposition of the deformation gradient in elastic and inelastic parts is assumed to apply. A yield function, related to the intermediate configuration is expressed in terms of the so-called Mandel stress tensor and a back stress tensor for kinematic hardening.
(ii) The constitutive equations for elastoplastic orthotropy are formulated in an invariant setting. So-called structural tensors describe the symmetries of the material in the elastic free energy function and the yield condition. The latter is expressed in terms of the invariants of the deviatoric part of the relative Mandel stresses and of the structural tensors.
(iii) The set of constitutive equations is solved by applying a general return method based on an operator split into an elastic predictor and a following corrector step. Plastic incompressibility is fulfilled exactly by means of the exponential map.
(iv) For finite element simulations of engineering problems in structural mechanics we use a formulation of a brick-type shell element, documented in [4], that overcomes artificial stiffening effects, called *locking*, by means of special interpolation techniques. Thus, the element is well suited for the numerical analysis of thin structures.
(v) We investigate two representative numerical examples: The necking of a circular bar for elastoplastic isotropy; for orthotropic material behavior we consider the bending of a circular plate.

2. Kinematics and constitutive framework

The considered body in the reference configuration is denoted by $\mathscr{B} \subset \mathbb{R}^3$. It is parametrized in $\mathbf{X}$ and the current configuration $\mathscr{S} \subset \mathbb{R}^3$ is parametrized in $\mathbf{x}$. The nonlinear deformation map $\boldsymbol{\varphi}_t : \mathscr{B} \to \mathscr{S}$ at time $t \in R_+$ maps points $\mathbf{X} \in \mathscr{B}$ onto points $\mathbf{x} \in \mathscr{S}$. Hence, the deformation gradient $\mathbf{F}$ is defined by $\mathbf{F}(\mathbf{X}) := \operatorname{Grad} \boldsymbol{\varphi}_t(\mathbf{X})$ with the Jacobian $J(\mathbf{X}) := \det \mathbf{F}(\mathbf{X}) > 0$. The index notation of $\mathbf{F}$ is $F^a_A := \partial x^a / \partial X^A$. Next, the right Cauchy–Green tensor is introduced by $\mathbf{C} = \mathbf{F}^{\mathrm{T}}\mathbf{F}$ with coefficients $C_{AB} = F^a_A F^b_B g_{ab}$, where g_{ab} denotes the coefficients of the covariant metric tensor in the current configuration.

2.1. Multiplicative elastoplasticity

Motivated by a micromechanical view of plastic deformations one postulates a multiplicative decomposition of the deformation gradient

$$\mathbf{F}(\mathbf{X}) = \mathbf{F}^{\mathrm{e}}(\mathbf{X})\mathbf{F}^{\mathrm{p}}(\mathbf{X}) \tag{1}$$

with the elastic and plastic parts $\mathbf{F}^{\mathrm{e}}$ and $\mathbf{F}^{\mathrm{p}}$, respectively. Eq. (1) implies a stress-free intermediate configuration, which is in general not compatible. It is well known that the decomposition is uniquely determined except for a rigid body rotation superposed on the intermediate configuration. Original references dealing with (1) can be found in the textbook [5]. Furthermore, the plastic incompressibility constraint

$$\det \mathbf{F}^{\mathrm{p}}(\mathbf{X}) = 1 \tag{2}$$

is assumed to hold. The constitutive equations are restricted by the second law of thermodynamics in the form of the Clausius–Duhem-inequality, which reads under the assumption of isothermal deformations with uniform temperature distribution

$$\mathscr{D} = \mathbf{S} : \dot{\mathbf{E}} - \dot{\psi} \geqslant 0. \tag{3}$$

In this local form the dissipation $\mathscr{D}$ denotes the difference between the stress power and the rate of the free energy per unit volume in the reference configuration. $\mathbf{S}$ and $\dot{\mathbf{E}}$ are the Second Piola–Kirchhoff stress tensor and the material time derivative of the Green–Lagrangian strain tensor $\mathbf{E} = \frac{1}{2}(\mathbf{C} - \mathbf{1})$, respectively. Here and in the following $\mathbf{1}$ denotes the second order unit tensor. Introducing the free energy $\psi = \psi(\mathbf{C}^{\mathrm{e}}, \boldsymbol{\chi})$ as a function of the elastic Right Cauchy–Green tensor $\mathbf{C}^{\mathrm{e}} := \mathbf{F}^{\mathrm{eT}}\mathbf{F}^{\mathrm{e}}$ and the internal variables $\boldsymbol{\chi}$—considered to be in general a set of tensors and scalars and represented as a vector—the associated rate is given by

$$\dot{\psi} = \frac{\partial \psi}{\partial \mathbf{C}^{\mathrm{e}}} : \dot{\mathbf{C}}^{\mathrm{e}} + \frac{\partial \psi}{\partial \boldsymbol{\chi}} \cdot \dot{\boldsymbol{\chi}}. \tag{4}$$

The strain rate $\dot{\mathbf{E}} = \frac{1}{2}\dot{\mathbf{C}}$ is derived by considering the multiplicative decomposition (1). One obtains, see e.g. [5],

$$\dot{\mathbf{C}} = \mathbf{F}^{\mathrm{p}\mathrm{T}}[\dot{\mathbf{C}}^{\mathrm{e}} + 2(\mathbf{C}^{\mathrm{e}}\mathbf{L}^{\mathrm{p}})_{\mathrm{s}}]\mathbf{F}^{\mathrm{p}} \quad \text{with } \mathbf{L}^{\mathrm{p}} = \dot{\mathbf{F}}^{\mathrm{p}}\mathbf{F}^{\mathrm{p}-1}, \tag{5}$$

where $\mathbf{L}^{\mathrm{p}}$ denotes the plastic velocity gradient and $(\ )_{\mathrm{s}}$ describes the symmetric part of a tensor. Since inequality (3), considering (4) and (5), must hold for all admissible processes in the material, standard arguments in rational thermodynamics with internal state variables yield the constitutive equations

$$\widehat{\mathbf{S}} = 2\frac{\partial \psi}{\partial \mathbf{C}^{\mathrm{e}}}, \quad \boldsymbol{\Xi} = \frac{\partial \psi}{\partial \boldsymbol{\chi}}. \tag{6}$$

Here, $\widehat{\mathbf{S}} = \mathbf{F}^{\mathrm{p}}\mathbf{S}\mathbf{F}^{\mathrm{p}\mathrm{T}}$ denotes the Second Piola–Kirchhoff stress tensor relative to the intermediate configuration and $\boldsymbol{\Xi}$ the internal stress vector conjugate to $\boldsymbol{\chi}$. Furthermore, one obtains the reduced local dissipation inequality

$$\mathscr{D} = \boldsymbol{\Sigma} : \mathbf{L}^{\mathrm{p}} - \boldsymbol{\Xi} \cdot \dot{\boldsymbol{\chi}} \geqslant 0, \tag{7}$$

where we call $\boldsymbol{\Sigma} := \mathbf{C}^{\mathrm{e}}\widehat{\mathbf{S}}$ the Mandel stress tensor, which for anisotropic elasticity is in general non-symmetric.

The evolution equations for the inelastic strain tensors can be derived by using the principle of maximum plastic dissipation. If the elastic domain E defined by the yield function $\Phi \leqslant 0$ is convex, a standard result in convex analysis shows, that, along with the loading–unloading conditions, the following normality rules for the rate equations of inelastic strains must hold:

$$\mathbf{L}^{\mathrm{p}} = \lambda \frac{\partial \Phi}{\partial \boldsymbol{\Sigma}}, \quad \dot{\boldsymbol{\chi}} = -\lambda \frac{\partial \Phi}{\partial \boldsymbol{\Xi}}. \tag{8}$$

In the following we specify the vector $\boldsymbol{\Xi}$ by introducing the scalar, stress-like hardening variable ξ and the back stress tensor $\hat{\boldsymbol{\beta}}$ for isotropic and kinematic hardening, respectively. Furthermore, we assume that the free energy function is additively decoupled in an elastic part ψ^{e}, a plastic part $\psi^{\mathrm{p,iso}}$ due to isotropic hardening and $\psi^{\mathrm{p,kin}}$ due to kinematic hardening of Melan–Prager type. The yield criterion Φ is formulated in terms of the relative stresses $\hat{\boldsymbol{\sigma}} := \boldsymbol{\Sigma} - \hat{\boldsymbol{\beta}}$ and the isotropic hardening stress ξ. According to (8) the evolution of the plastic deformation gradient $\mathbf{F}^{\mathrm{p}}$ and of the internal variables $\boldsymbol{\chi}$ are given with Φ as a plastic potential. Here, $\boldsymbol{\chi}$ contains the tensor valued $\boldsymbol{\alpha}$, conjugate to the back stress $\hat{\boldsymbol{\beta}}$ as well as the scalar-valued equivalent plastic strain e^{p}, conjugate to ξ.

2.2. Isotropic tensor functions for the representation of anisotropic material response

In case of anisotropy we introduce a material symmetry group $\mathscr{G}_k$ characterizing the anisotropy class of the material. $\mathscr{G}_k$ is defined with respect to the reference configuration, and we assume that it remains unchanged during plastic deformations. The elements of $\mathscr{G}_k$ are denoted by the unimodular tensors ${}^{i}\mathbf{Q}|_{i=1,\ldots,n}$. Here, the concept of material symmetry will be formulated for an orthotropic elasticity law, which is related to the intermediate configuration and therefore is expressed in terms of the elastic Green strain tensor $\widehat{\mathbf{E}}^{\mathrm{e}} = (\mathbf{C}^{\mathrm{e}} - \mathbf{1})/2$. Based on our assumption this concept requires that the elastic material response must be invariant under transformations on the intermediate configuration with elements of the symmetry group $\mathscr{G}_k$

$$\hat{\psi}^{\mathrm{e}}(\mathbf{Q}^{\mathrm{T}}\widehat{\mathbf{E}}^{\mathrm{e}}\mathbf{Q}) = \hat{\psi}^{\mathrm{e}}(\widehat{\mathbf{E}}^{\mathrm{e}}) \quad \forall \mathbf{Q} \in \mathscr{G}_k, \widehat{\mathbf{E}}^{\mathrm{e}}. \tag{9}$$

We call the function ψ^{e} a $\mathscr{G}_k$-invariant function. Without any restrictions for solid materials we set $\mathscr{G}_k \subset \mathrm{SO}(3)$. Based on the mapping $\widehat{\mathbf{X}} \to \mathbf{Q}^{\mathrm{T}}\widehat{\mathbf{X}}$, applied to the intermediate configuration $\widehat{\mathbf{X}}$, for arbitrary rotation tensors $\mathbf{Q} \in \mathrm{SO}(3)$ we have, in view of a coordinate free representation, to fulfill the transformation rule $\mathbf{Q}^{\mathrm{T}}\widehat{\mathbf{S}}(\widehat{\mathbf{E}}^{\mathrm{e}}, \bullet)\mathbf{Q} = \widehat{\mathbf{S}}(\mathbf{Q}^{\mathrm{T}}\widehat{\mathbf{E}}^{\mathrm{e}}\mathbf{Q}, \bullet)$ $\forall \mathbf{Q} \in \mathrm{SO}(3)$, where $(\bullet)$ denotes additional tensor arguments. In order to construct an isotropic tensor function for the anisotropic constitutive behavior, the $\mathscr{G}_k$-invariant function must be extended in a manner, that it becomes invariant under the special orthogonal group; this is done by the introduction of the so-called structural tensors reflecting the material symmetries. Recall here, that a second order tensor $\mathbf{M}$ is a structural tensor of an anisotropic material characterized by a symmetry group $\mathscr{G}_k$ if $\mathbf{Q}^{\mathrm{T}}\mathbf{M}\mathbf{Q} = \mathbf{M}$ for all $\mathbf{Q} \in \mathscr{G}_k$. Orthotropic materials can be characterized by

three symmetry planes, described by three structural tensors ${}^{i}\mathbf{M}|_{i=1,2,3}$. Thus, the constitutive equation can be expressed as an isotropic scalar-valued tensor function in the arguments $(\widehat{\mathbf{E}}^{\mathrm{e}}, {}^{1}\mathbf{M}, {}^{2}\mathbf{M}, {}^{3}\mathbf{M})$ in the form

$$\hat{\psi}^{\mathrm{e}}(\widehat{\mathbf{E}}^{\mathrm{e}}, {}^{i}\mathbf{M}|_{i=1,2,3}) = \hat{\psi}^{\mathrm{e}}(\mathbf{Q}^{\mathrm{T}}\widehat{\mathbf{E}}^{\mathrm{e}}\mathbf{Q}, \mathbf{Q}^{\mathrm{T}}{}^{i}\mathbf{M}\mathbf{Q}|_{i=1,2,3}) \quad \forall \mathbf{Q} \in \mathrm{SO}(3), \tag{10}$$

which fulfills the above postulated transformation rule for the stresses.

2.3. Orthotropic elastic free energy function

The material symmetry group of the considered orthotropic material is defined by $\mathscr{G}_o := \{\mathbf{I}; \mathbf{S}_1, \mathbf{S}_2, \mathbf{S}_3\}$, where $\mathbf{S}_1$, $\mathbf{S}_2$, $\mathbf{S}_3$ are the reflections with respect to the basis planes $({}^{2}\mathbf{a}, {}^{3}\mathbf{a})$, $({}^{3}\mathbf{a}, {}^{1}\mathbf{a})$ and $({}^{1}\mathbf{a}, {}^{2}\mathbf{a})$, respectively. Here, $({}^{1}\mathbf{a}, {}^{2}\mathbf{a}, {}^{3}\mathbf{a})$ represents an orthonormal privileged frame. Based on this, we obtain for this symmetry group the three structural tensors

$${}^{1}\mathbf{M} := {}^{1}\mathbf{a} \otimes {}^{1}\mathbf{a}, \quad {}^{2}\mathbf{M} := {}^{2}\mathbf{a} \otimes {}^{2}\mathbf{a} \quad \text{and} \quad {}^{3}\mathbf{M} := {}^{3}\mathbf{a} \otimes {}^{3}\mathbf{a}, \tag{11}$$

which represent the orthotropic material symmetry. Due to the fact that the sum of the three structural tensors yields $\sum_{i=1}^{3} {}^{i}\mathbf{M} = \mathbf{1}$ we may discard ${}^{3}\mathbf{M}$ from the set of structural tensors (11). The integrity basis is given by $\mathscr{P} := \{J_1, \ldots, J_7\}$. The invariants J_1, J_2, J_3 are defined by the traces of powers of $\widehat{\mathbf{E}}^{\mathrm{e}}$, i.e.,

$$J_1 := \operatorname{tr}\widehat{\mathbf{E}}^{\mathrm{e}}, \quad J_2 := \operatorname{tr}[(\widehat{\mathbf{E}}^{\mathrm{e}})^2], \quad J_3 := \operatorname{tr}[(\widehat{\mathbf{E}}^{\mathrm{e}})^3]. \tag{12}$$

The irreducible mixed invariants are given by

$$\left.\begin{aligned} J_4 &:= \operatorname{tr}[{}^{1}\mathbf{M}\widehat{\mathbf{E}}^{\mathrm{e}}], \quad J_5 := \operatorname{tr}[{}^{1}\mathbf{M}(\widehat{\mathbf{E}}^{\mathrm{e}})^2] \\ J_6 &:= \operatorname{tr}[{}^{2}\mathbf{M}\widehat{\mathbf{E}}^{\mathrm{e}}], \quad J_7 := \operatorname{tr}[{}^{2}\mathbf{M}(\widehat{\mathbf{E}}^{\mathrm{e}})^2] \end{aligned}\right\}, \tag{13}$$

see e.g. [3]. For ψ^{e} we assume a quadratic form, viz.,

$$\psi^{\mathrm{e}} = \tfrac{1}{2}\lambda J_1^2 + \mu J_2 + \tfrac{1}{2}\alpha_1 J_4^2 + \tfrac{1}{2}\alpha_2 J_6^2 + 2\alpha_3 J_5 + 2\alpha_4 J_7 + \alpha_5 J_4 J_1 + \alpha_6 J_6 J_1 + \alpha_7 J_4 J_6. \tag{14}$$

For the Second Piola–Kirchhoff stresses related to the intermediate configuration we have

$$\left.\begin{aligned} \widehat{\mathbf{S}} = {} & \lambda J_1 \mathbf{1} + 2\mu\widehat{\mathbf{E}}^{\mathrm{e}} + \alpha_1 J_4 {}^{1}\mathbf{M} + \alpha_2 J_6 {}^{2}\mathbf{M} + 2\alpha_3\left(\widehat{\mathbf{E}}^{\mathrm{e}}{}^{1}\mathbf{M} + {}^{1}\mathbf{M}\widehat{\mathbf{E}}^{\mathrm{e}}\right) \\ & + 2\alpha_4\left(\widehat{\mathbf{E}}^{\mathrm{e}}{}^{2}\mathbf{M} + {}^{2}\mathbf{M}\widehat{\mathbf{E}}^{\mathrm{e}}\right) + \alpha_5(J_1 {}^{1}\mathbf{M} + J_4\mathbf{1}) \\ & + \alpha_6(J_1 {}^{2}\mathbf{M} + J_6\mathbf{1}) + \alpha_7(J_4 {}^{2}\mathbf{M} + J_6 {}^{1}\mathbf{M}) \end{aligned}\right\}. \tag{15}$$

In this special case the second derivative of ψ^{e} yields the constant fourth-order elasticity tensor

$$\left.\begin{aligned} \mathbb{C}^{\mathrm{e}} = {} & \lambda\mathbf{1}\otimes\mathbf{1} + 2\mu\mathbb{I} + \alpha_1 {}^{1}\mathbf{M}\otimes{}^{1}\mathbf{M} + \alpha_2 {}^{2}\mathbf{M}\otimes{}^{2}\mathbf{M} \\ & + 2\alpha_3\mathbb{K}_1 + 2\alpha_4\mathbb{K}_2 + \alpha_5({}^{1}\mathbf{M}\otimes\mathbf{1} + \mathbf{1}\otimes{}^{1}\mathbf{M}) \\ & + \alpha_6({}^{2}\mathbf{M}\otimes\mathbf{1} + \mathbf{1}\otimes{}^{2}\mathbf{M}) + \alpha_7({}^{2}\mathbf{M}\otimes{}^{1}\mathbf{M} + {}^{1}\mathbf{M}\otimes{}^{2}\mathbf{M}) \end{aligned}\right\} \tag{16}$$

with $\mathbb{I}_{IJKL} = \delta_{IK}\delta_{JL}$, $\mathbb{K}^1_{IJKL} = \delta_{IK}{}^{1}M_{JL} + \delta_{JL}{}^{1}M_{IK}$ and $\mathbb{K}^2_{IJKL} = \delta_{IK}{}^{2}M_{JL} + \delta_{JL}{}^{2}M_{IK}$. The elasticity parameters $(\lambda, \mu, \alpha_i | i = 1, \ldots, 7)$ can be identified using the matrix notation

$$\begin{bmatrix} \widehat{S}_{11} \\ \widehat{S}_{22} \\ \widehat{S}_{33} \\ \widehat{S}_{12} \\ \widehat{S}_{13} \\ \widehat{S}_{23} \end{bmatrix} = \begin{bmatrix} \mathbb{C}_{11} & \mathbb{C}_{12} & \mathbb{C}_{13} & 0 & 0 & 0 \\ \mathbb{C}_{12} & \mathbb{C}_{22} & \mathbb{C}_{23} & 0 & 0 & 0 \\ \mathbb{C}_{13} & \mathbb{C}_{23} & \mathbb{C}_{33} & 0 & 0 & 0 \\ 0 & 0 & 0 & \mathbb{C}_{44} & 0 & 0 \\ 0 & 0 & 0 & 0 & \mathbb{C}_{55} & 0 \\ 0 & 0 & 0 & 0 & 0 & \mathbb{C}_{66} \end{bmatrix} \begin{bmatrix} \widehat{E}^{\mathrm{e}}_{11} \\ \widehat{E}^{\mathrm{e}}_{22} \\ \widehat{E}^{\mathrm{e}}_{33} \\ 2\widehat{E}^{\mathrm{e}}_{12} \\ 2\widehat{E}^{\mathrm{e}}_{13} \\ 2\widehat{E}^{\mathrm{e}}_{23} \end{bmatrix} \tag{17}$$

with the elasticity constants $\mathbb{C}_{ij}$. Choosing the preferred directions as ${}^{1}\mathbf{a} = (1,0,0)^{\mathrm{T}}$ and ${}^{2}\mathbf{a} = (0,1,0)^{\mathrm{T}}$ we obtain the material parameters λ, μ, α_1, α_2, α_3, α_4, α_5, α_6 in terms of components $\mathbb{C}_{ij}$. In case of isotropy the only remaining constants are λ and μ.

2.4. Orthotropic yield criterion

In the following, we consider an orthotropic pressure insensitive yield condition using isotropic tensor functions. It is assumed that Φ depends on the symmetric part of the relative stresses $\hat{\boldsymbol{\sigma}}_{\mathrm{s}} := (\boldsymbol{\Sigma} - \hat{\boldsymbol{\beta}})_{\mathrm{s}}$ only. As a consequence the following relations hold for the plastic velocity gradients:

$$\mathbf{L}^{\mathrm{p}} = \mathbf{L}^{\mathrm{pT}}, \quad \mathbf{D}^{\mathrm{p}} := \operatorname{sym}(\mathbf{L}^{\mathrm{p}}) = \mathbf{L}^{\mathrm{p}}, \quad \mathbf{W}^{\mathrm{p}} := \operatorname{skew}(\mathbf{L}^{\mathrm{p}}) = \mathbf{0}. \tag{18}$$

This assumption and its implications will be discussed below.

The integrity basis in terms of the deviatoric part of the relative stresses $\operatorname{dev}\hat{\boldsymbol{\sigma}}_s$ and the structural tensors ${}^1\mathbf{M}$ and ${}^2\mathbf{M}$ is given by

$$\left.\begin{aligned} I_1 &:= \operatorname{tr}[(\operatorname{dev}\hat{\boldsymbol{\sigma}}_s)^2], & I_2 &:= \operatorname{tr}[{}^1\mathbf{M}(\operatorname{dev}\hat{\boldsymbol{\sigma}}_s)^2],\\ I_3 &:= \operatorname{tr}[{}^2\mathbf{M}(\operatorname{dev}\hat{\boldsymbol{\sigma}}_s)^2], & I_4 &:= \operatorname{tr}[{}^1\mathbf{M}\operatorname{dev}\hat{\boldsymbol{\sigma}}_s],\\ I_5 &:= \operatorname{tr}[{}^2\mathbf{M}\operatorname{dev}\hat{\boldsymbol{\sigma}}_s], & I_6 &:= \operatorname{tr}[(\operatorname{dev}\hat{\boldsymbol{\sigma}}_s)^3]. \end{aligned}\right\} \tag{19}$$

The orthotropic flow criterion is formulated as an isotropic tensor function

$$\widehat{\boldsymbol{\Phi}}(\operatorname{dev}\hat{\boldsymbol{\sigma}}_s, {}^1\mathbf{M}, {}^2\mathbf{M}) = \widehat{\boldsymbol{\Phi}}(\mathbf{Q}^{\mathrm{T}}\operatorname{dev}\hat{\boldsymbol{\sigma}}_s\mathbf{Q}, \mathbf{Q}^{\mathrm{T}}{}^1\mathbf{M}\mathbf{Q}, \mathbf{Q}^{\mathrm{T}}{}^2\mathbf{M}\mathbf{Q}) \quad \forall \mathbf{Q} \in \mathrm{SO}(3). \tag{20}$$

Discarding the cubic invariant I_6 in Φ we arrive at a quadratic form in terms of the invariants and six independent material parameters $\eta_i|_{i=1,\ldots,6}$, respectively

$$\Phi = \eta_1 I_1 + \eta_2 I_2 + \eta_3 I_3 + \eta_4 I_4^2 + \eta_5 I_5^2 + \eta_6 I_4 I_5 - \left(1 + \frac{\hat{\xi}(e^{\mathrm{p}})}{Y_{11}^0}\right)^2. \tag{21}$$

Remark. It can be shown, see [6–8], that under rigid body rotations $\mathbf{Q}$ superposed on the current configuration and—simultaneously—rigid body rotations $\overline{\mathbf{Q}}$ on the intermediate configuration the following transformation rules apply

$$\begin{aligned} &\mathbf{F} \to \mathbf{F}^* = \mathbf{Q}\mathbf{F} = \mathbf{Q}\mathbf{F}^{\mathrm{e}}\overline{\mathbf{Q}}^{\mathrm{T}}\overline{\mathbf{Q}}\mathbf{F}^{\mathrm{p}} = \mathbf{Q}\overline{\mathbf{F}}^{\mathrm{e}}\overline{\mathbf{F}}^{\mathrm{p}},\\ &(\ ) \to (\ )^* = \overline{\mathbf{Q}}(\ )\overline{\mathbf{Q}}^{\mathrm{T}} \quad \text{for } \mathbf{C}^{\mathrm{e}}, \widehat{\mathbf{S}}, \boldsymbol{\Sigma}, \mathbf{D}^{\mathrm{p}},\\ &\mathbf{L}^{\mathrm{p}} \to \mathbf{L}^{\mathrm{p}*} = \overline{\mathbf{Q}}\mathbf{L}^{\mathrm{p}}\overline{\mathbf{Q}}^{\mathrm{T}} + \dot{\overline{\mathbf{Q}}}\overline{\mathbf{Q}}^{\mathrm{T}}, \end{aligned} \tag{22}$$

where we have restricted ourselves to tensorial quantities of the intermediate configuration playing an eminent role in the present formulation. Invariance of constitutive equations under rigid body rotations superposed on the current configuration is generally required by the principle of material frame indifference, the latter invariance requirement is due to the well known fact, that the multiplicative decomposition is uniquely defined except for a rigid body rotation superposed on the intermediate configuration; the identity $\overline{\mathbf{Q}}^{\mathrm{T}}\overline{\mathbf{Q}}$ can always be inserted, in between $\mathbf{F}^{\mathrm{e}}$ and $\mathbf{F}^{\mathrm{p}}$, see $(22)_1$. As a consequence of the constitutive assumption, that only the symmetric part $\hat{\boldsymbol{\sigma}}_s$ enters the yield function, the flow rule reads $\mathbf{D}^{\mathrm{p}} = \lambda\partial_{\boldsymbol{\Sigma}_s}\Phi$, which is, see $(22)_2$, invariant with respect to the arbitrary choice of $\overline{\mathbf{Q}}$, whereas this is not true for the plastic velocity gradient $\mathbf{L}^{\mathrm{p}}$ due to the expression $\dot{\overline{\mathbf{Q}}}\overline{\mathbf{Q}}^{\mathrm{T}}$ in $(22)_3$.

As a further consequence of the yield function in terms of $\hat{\boldsymbol{\sigma}}_s$ the six independent material parameters $\eta_i|_{i=1,\ldots,6}$ can be experimentally identified by three tension tests and three shear tests, respectively, which are independent of each other.

Each test leads to a set of values for the invariants. Evaluating the flow criterion for all six distinct tests yields a system of linear equations with the solution $\eta_i|_{i=1,\ldots,6}$, which are each functions in terms of the physical yield stresses.

The constitutive equations are now summarized as follows:

$$\begin{aligned} &\text{elastic strains} && \mathbf{C}^{\mathrm{e}} = \mathbf{F}^{\mathrm{pT}-1}\mathbf{C}\mathbf{F}^{\mathrm{p}-1},\\ &\text{free energy} && \psi = \hat{\psi}^{\mathrm{e}}(J_1,\ldots,J_6) + \hat{\psi}^{\mathrm{p,iso}}(e^{\mathrm{p}}) + \hat{\psi}^{\mathrm{p,kin}}(\boldsymbol{\alpha}),\\ &\text{stresses} && \widehat{\mathbf{S}} = 2\partial_{C^{\mathrm{e}}}\psi^{\mathrm{e}}, \quad \boldsymbol{\Sigma} = \mathbf{C}^{\mathrm{e}}\widehat{\mathbf{S}},\\ &\text{back stresses} && \hat{\boldsymbol{\beta}} = \partial_{\alpha}\psi^{\mathrm{p,kin}},\\ &\text{isotropic hardening} && \xi = \partial_{e^{\mathrm{p}}}\psi^{\mathrm{p,iso}},\\ &\text{relative stresses} && \hat{\boldsymbol{\sigma}}_s = \boldsymbol{\Sigma}_s - \hat{\boldsymbol{\beta}}_s,\\ &\text{yield function} && \Phi = \hat{\Phi}(I_1,\ldots,I_5,\xi),\\ &\text{associated flow rule} && \mathbf{D}^{\mathrm{p}} = \lambda\partial_{\boldsymbol{\Sigma}_s}\Phi,\\ &\text{evolution of } \boldsymbol{\alpha} && \dot{\boldsymbol{\alpha}} = -\lambda\partial_{\hat{\beta}_s}\Phi,\\ &\text{evolution of } e^{\mathrm{p}} && \dot{e}^{\mathrm{p}} = \sqrt{\frac{2}{3}}\|\mathbf{D}^{\mathrm{p}}\|,\\ &\text{optimization conditions} && \lambda \geqslant 0,\ \Phi \leqslant 0,\ \lambda\Phi = 0. \end{aligned} \tag{23}$$

Now we consider pure isotropy as a special case of orthotropy. For isotropic elasticity $\boldsymbol{\Sigma} = \boldsymbol{\Sigma}^{\mathrm{T}}$ holds and therefore $\mathbf{L}^{\mathrm{p}} = \mathbf{D}^{\mathrm{p}}$. In this case our constitutive assumption for Φ being a function merely of the symmetric part of $\boldsymbol{\Sigma}$ is fulfilled by the elasticity law itself. If we set for the yield normal stresses $Y_{ii}^0 = Y^0$ for $i = 1,2,3$ and for the yield shear stresses $Y_{ij}^0 = Y^0/\sqrt{3}$ for $i \neq j$ with $i,j = 1,2,3$ we arrive at the isotropic von Mises yield criterion

$$\hat{\Phi}(\operatorname{dev}\hat{\boldsymbol{\sigma}},\xi)=\frac{3}{2}\left(\frac{\|\operatorname{dev}\hat{\boldsymbol{\sigma}}\|}{Y^0}\right)^2-\left(1+\frac{\hat{\xi}(e^{\mathrm{p}})}{Y^0}\right)^2\leqslant 0. \tag{24}$$

In one of the computational benchmark problems in Section 5 we apply a nonlinear isotropic hardening function well suited for a fitting of experimental data

$$\hat{\xi}(e^{\mathrm{p}})=he^{\mathrm{p}}+(Y^{\infty}-Y^0)(1-\exp(-\delta e^{\mathrm{p}})), \tag{25}$$

where h is the linear hardening parameter and where the expression in terms of Y^{∞}, Y^0 and δ in (25) is of saturation type.

3. Integration algorithm and algorithmic elastoplastic moduli

To solve the set of constitutive equations at a local level, a so-called operator split along with a general return mapping is applied; for time integration a backward Euler scheme with an exponential map is used. For the solution of the nonlinear finite element equations on a global level a Newton iteration scheme is used, which requires the consistent tangent matrix. For this reason a simple numerical differentiation technique is applied.

Based on the definition $(5)_2$ of $\mathbf{L}^{\mathrm{p}}$, and taking $\mathbf{L}^{\mathrm{p}}=\mathbf{D}^{\mathrm{p}}$ into account, we write the flow rule $(23)_8$ for $\mathbf{D}^{\mathrm{p}}$ as

$$\dot{\mathbf{F}}^{\mathrm{p}}=\mathbf{D}^{\mathrm{p}}\mathbf{F}^{\mathrm{p}}=\lambda\mathbf{N}\mathbf{F}^{\mathrm{p}}\quad\text{with }\mathbf{N}:=\frac{\partial\Phi}{\partial\boldsymbol{\Sigma}_{\mathrm{s}}}. \tag{26}$$

Within a typical time step $[t_n,t_{n+1}]$ with time increment $\Delta t:=t_{n+1}-t_n$ we integrate (26) by the implicit backward Euler algorithm along with an exponential shift

$$\mathbf{F}^{\mathrm{p}}_{n+1}=\exp[\gamma\partial_{\Sigma_{\mathrm{s}}}\Phi_{n+1}]\mathbf{F}^{\mathrm{p}}_n, \tag{27}$$

where $\gamma:=\Delta t\lambda_{n+1}$ denotes the consistency parameter. For $\mathbf{N}$ we use the corresponding tensor of the trial step defined below. For deviatoric $\mathbf{N}$, i.e. $\operatorname{tr}[\mathbf{N}]=0$, and applying the identity $\det(\exp[\mathbf{N}])=\exp[\operatorname{tr}(\mathbf{N})]$, it is obvious that the exponential map (27) preserves plastic incompressibility in the current time step, given that $\det\mathbf{F}^{\mathrm{p}}_n=1$ holds for the previous step. The rate equations for $\boldsymbol{\alpha}$ and e^{p} are integrated using a standard backward Euler algorithm. Thus, the procedure for time integration is first order accurate and unconditionally stable. Considering the multiplicative decomposition we obtain for the update of the elastic Cauchy–Green tensor

$$\begin{aligned}\mathbf{C}^{\mathrm{e}}_{n+1}&=\mathbf{F}^{\mathrm{pT}-1}_{n+1}\mathbf{C}_{n+1}\mathbf{F}^{\mathrm{p}-1}_{n+1}\\&=\exp^{\mathrm{T}}[-\gamma_{n+1}\mathbf{N}^{\mathrm{trial}}_{n+1}]\mathbf{C}^{\mathrm{e\ trial}}_{n+1}\exp[-\gamma_{n+1}\mathbf{N}^{\mathrm{trial}}_{n+1}],\end{aligned} \tag{28}$$

where we have introduced by definition $\mathbf{C}^{\mathrm{e\ trial}}_{n+1}:=\mathbf{F}^{\mathrm{pT}-1}_{n}\mathbf{C}_{n+1}\mathbf{F}^{\mathrm{p}-1}_{n}$ as elastic trial strains. It is well known that for the case of isotropic elasticity $\mathbf{N}_{n+1}$ and $\mathbf{C}^{\mathrm{e}}_{n+1}$ commute, i.e. they have the same principal directions, which allows for a stress update formula that is identical to the classical return mapping algorithm of the geometrically linear theory, see [9,10].

With the trial values for the Mandel stresses $\boldsymbol{\Sigma}^{\mathrm{trial}}_{n+1}=2\mathbf{C}^{\mathrm{e\ trial}}_{n+1}\partial_{\mathbf{C}^{\mathrm{e\ trial}}_{n+1}}\psi^{\mathrm{e}}$, and for the internal variables, i.e. the back stresses $\hat{\boldsymbol{\beta}}^{\mathrm{trial}}_{n+1}=\partial_{\boldsymbol{\alpha}_n}\psi^{\mathrm{p,kin}}$ and the equivalent plastic strain $e^{\mathrm{p\ trial}}_{n+1}=\partial_{\xi_n}\psi^{\mathrm{p,iso}}$ we obtain a trial value for the yield criterion in terms of the deviatoric part of the symmetric relative stresses $\operatorname{dev}\hat{\boldsymbol{\sigma}}_{\mathrm{s}}$ as follows:

$$\Phi^{\mathrm{trial}}_{n+1}=\hat{\Phi}(\operatorname{dev}\hat{\boldsymbol{\sigma}}^{\mathrm{trial}}_{\mathrm{s}},{}^{i}\mathbf{M},e^{\mathrm{p}}_n)^{\mathrm{trial}}_{n+1}. \tag{29}$$

The time discrete consistency condition reads in the case of plastic loading $\Phi_{n+1}=0$, which can be solved for γ_{n+1} by applying a Newton solution scheme. At the end of each local iteration the intermediate configuration, described by $\mathbf{F}^{\mathrm{p}}_{n+1}$, and the internal variables $\boldsymbol{\alpha}_{n+1}$ and e^{p}_{n+1} have to be updated. A summary of the general return mapping algorithm is given in (33).

As we use a Lagrangian formulation of the weak form, which is outlined in Section 4, the Second Piola–Kirchhoff stress tensor must be determined by pull back transformation $\mathbf{S}=\mathbf{F}^{\mathrm{p}-1}\widehat{\mathbf{S}}\mathbf{F}^{\mathrm{pT}-1}$. The nonlinear finite-element equations are solved by using a Newton iteration scheme. For this purpose the so-called consistent tangent matrix

$$\mathbb{C}_{\mathrm{ep}}=2\partial\mathbf{S}/\partial\mathbf{C}=\mathbb{C}^{ABCD}\mathbf{e}_A\otimes\mathbf{e}_B\otimes\mathbf{e}_C\otimes\mathbf{e}_D \tag{30}$$

is approximated by numerical differentiation. To this end a simple perturbation technique is applied using the forward difference formula

$$\mathbb{C}^{ABCD} \approx \frac{2}{\epsilon}\left[S^{AB}(\mathbf{C}^{\epsilon}_{(CD)}) - S^{AB}\right]. \tag{31}$$

The perturbed Cauchy–Green tensor is computed as

$$\mathbf{C}^{\epsilon}_{(CD)} := \mathbf{C} + \Delta\mathbf{C}^{\epsilon}_{(CD)} \quad \text{with}$$
$$\Delta\mathbf{C}^{\epsilon}_{(CD)} = \frac{\epsilon}{2}(\mathbf{e}_C \otimes \mathbf{e}_D + \mathbf{e}_D \otimes \mathbf{e}_C), \tag{32}$$

where $\mathbf{e}_I$, $I = A, B, C, D$ denotes a fixed Cartesian basis. Computations have shown, that $\epsilon = 10^{-7}$ provides a good choice for the perturbation parameter. As the numerical differentiation requires six additional stress computations, it costs more CPU time than the analytical computation of the moduli. Nevertheless, the numerical determination of consistent algorithmic moduli is advantageous for its simplicity, robustness and for being independent of the material model. It serves as an interface for implementing complicated constitutive models without tedious analytical derivations of tangent operators.

1. Trial step : elastic predictor

$$\mathbf{C}^{\mathrm{e\,trial}}_{n+1} = \mathbf{F}^{\mathrm{pT}-1}_{n}\mathbf{C}_{n+1}\mathbf{F}^{\mathrm{p}-1}_{n}$$
$$\boldsymbol{\Sigma}^{\mathrm{trial}}_{n+1} = 2\mathbf{C}^{\mathrm{e\,trial}}_{n+1}\frac{\partial\psi^{\mathrm{e}}}{\partial\mathbf{C}^{\mathrm{e\,trial}}_{n+1}}, \quad \hat{\boldsymbol{\beta}}^{\mathrm{trial}}_{n+1} = \frac{\partial\psi^{\mathrm{p,kin}}}{\partial\boldsymbol{\alpha}_n}$$
$$\hat{\boldsymbol{\sigma}}^{\mathrm{trial}}_{n+1} := \boldsymbol{\Sigma}^{\mathrm{trial}}_{n+1} - \hat{\boldsymbol{\beta}}^{\mathrm{trial}}_{n+1}, \quad \mathbf{N}^{\mathrm{trial}}_{n+1} = \frac{\partial\Phi}{\partial\boldsymbol{\Sigma}^{\mathrm{trial}}_{\mathrm{s}\,n+1}}$$

2. Check yield condition

if $\widehat{\Phi}(\mathrm{dev}\,\hat{\boldsymbol{\sigma}}^{\mathrm{trial}}_{\mathrm{s}\,n+1}, {}^{i}\mathbf{M}, e^{\mathrm{p}}_{n}) > 0$ go to 3.
else exit

3. Return mapping : corrector step

set $\gamma^{(0)}_{n+1} = 0, \quad e^{\mathrm{p}(0)}_{n+1} = e^{\mathrm{p}}_{n}, \quad \boldsymbol{\alpha}^{(0)}_{n+1} = \boldsymbol{\alpha}_n$

(a) $\mathbf{C}^{\mathrm{e}(l)}_{n+1} = \exp^{\mathrm{T}}[-\gamma^{(l)}_{n+1}\mathbf{N}^{\mathrm{trial}}_{n+1}]\mathbf{C}^{\mathrm{e\,trial}}_{n+1}\exp[-\gamma^{(l)}_{n+1}\mathbf{N}^{\mathrm{trial}}_{n+1}]$
$e^{\mathrm{p}(l)}_{n+1} = e^{\mathrm{p}}_{n} + \gamma^{(l)}_{n+1}\sqrt{\frac{2}{3}}\|\mathbf{N}^{\mathrm{trial}}_{n+1}\|,$
$\boldsymbol{\alpha}^{(l)}_{n+1} = \boldsymbol{\alpha}_n + \gamma^{(l)}_{n+1}\mathbf{N}^{\mathrm{trial}}_{n+1}$

(b) $\boldsymbol{\Sigma}^{(l)}_{n+1} = 2\mathbf{C}^{\mathrm{e}(l)}_{n+1}\frac{\partial\psi^{\mathrm{e}}}{\partial\mathbf{C}^{\mathrm{e}(l)}_{n+1}}, \quad \hat{\boldsymbol{\beta}}^{(l)}_{n+1} = \frac{\partial\psi^{\mathrm{p,kin}}}{\partial\boldsymbol{\alpha}^{(l)}_{n+1}},$
$\xi^{(l)}_{n+1} = \frac{\partial\psi^{\mathrm{p,iso}}}{\partial e^{\mathrm{p}(l)}_{n+1}}$

(c) $\Phi^{(l)}_{n+1} = \Phi(\gamma^{(l)}_{n+1}),$
$\Phi'^{(l)}_{n+1} \approx [\Phi(\gamma^{(l)}_{n+1} + \epsilon) - \Phi(\gamma^{(l)}_{n+1})]/\epsilon$
if $|\Phi^{(l)}_{n+1}| \leqslant \mathrm{tol}$ go to 4.

(d) $\gamma^{(l+1)}_{n+1} = \gamma^{(l)}_{n+1} - \Phi^{(l)}_{n+1}/\Phi'^{(l)}_{n+1}$ go to (a)

4. Update intermediate configuration and internal variables

$$\mathbf{F}^{\mathrm{p}}_{n+1} = \exp[\gamma^{(l)}_{n+1}\mathbf{N}^{\mathrm{trial}}_{n+1}]\mathbf{F}^{\mathrm{p}}_{n}, \quad e^{\mathrm{p}}_{n+1} = e^{\mathrm{p}(l)}_{n+1},$$
$$\boldsymbol{\alpha}_{n+1} = \boldsymbol{\alpha}^{(l)}_{n+1} \tag{33}$$

Remark. For an efficient computation of the exponential function of a (generally nonsymmetric) second order tensor we use an recursive algorithm, see [11,12].

4. Variational formulation

Let $\mathscr{B}$ be the reference body of interest which is bounded by the surface $\partial\mathscr{B}$. The surface is partitioned into two disjoint parts $\partial\mathscr{B} = \partial\mathscr{B}_u \bigcup \partial\mathscr{B}_t$ with $\partial\mathscr{B}_u \bigcap \partial\mathscr{B}_t = \emptyset$. The equation of balance of linear momentum for the static case is governed by the First Piola–Kirchhoff stresses $\mathbf{P} = \mathbf{FS}$ and the body force $\hat{\mathbf{b}}$ in the reference configuration

$$\mathrm{Div}[\mathbf{FS}] + \hat{\mathbf{b}} = \mathbf{0}. \tag{34}$$

The Dirichlet and Neumann boundary conditions are given by $\mathbf{u} = \bar{\mathbf{u}}$ on $\partial\mathscr{B}_u$ and $\mathbf{t} = \hat{\mathbf{t}} = \mathbf{PN}$ on $\partial\mathscr{B}_t$. With standard arguments of variational calculus we arrive at

$$G(\mathbf{u}, \delta\mathbf{u}) = \int_{\mathscr{B}} \mathbf{S} : \delta\mathbf{E}\,\mathrm{d}V + G^{\mathrm{ext}} \tag{35}$$

with

$$G^{\mathrm{ext}}(\delta\mathbf{u}) := -\int_{\mathscr{B}} \hat{\mathbf{b}}\cdot\delta\mathbf{u}\,\mathrm{d}V - \int_{\partial\mathscr{B}_t} \hat{\mathbf{t}}\cdot\delta\mathbf{u}\,\mathrm{d}A, \tag{36}$$

where $\delta\mathbf{E} := \frac{1}{2}(\delta\mathbf{F}^{\mathrm{T}}\mathbf{F} + \mathbf{F}^{\mathrm{T}}\delta\mathbf{F})$ characterizes the virtual Green–Lagrangian strain tensor in terms of the virtual deformation gradient $\delta\mathbf{F} := \mathrm{Grad}\,\delta\mathbf{u}$. The equation of principle of virtual work (35) for a static equilibrium state of the considered body requires $G = 0$. For the solution of this nonlinear equation a standard Newton iteration scheme is

applied, which requires the consistent linearization of (35) in order to guarantee quadratic convergence rate near the solution. Since the stress tensor $\mathbf{S}$ is symmetric, the linear increment of G denoted by ΔG is given by

$$\Delta G(\mathbf{u}, \delta\mathbf{u}, \Delta\mathbf{u}) := \int_{\mathscr{B}} (\delta\mathbf{E} : \Delta\mathbf{S} + \Delta\delta\mathbf{E} : \mathbf{S}) \mathrm{d}V, \quad (37)$$

where $\Delta\delta\mathbf{E} := \frac{1}{2}(\Delta\mathbf{F}^{\mathrm{T}}\delta\mathbf{F} + \delta\mathbf{F}^{\mathrm{T}}\Delta\mathbf{F})$ denotes the linearized virtual Green–Lagrange strain tensor as a function of the incremental deformation gradient $\Delta\mathbf{F} := \mathrm{Grad}\,\Delta\mathbf{u}$. The incremental Second Piola–Kirchhoff stress tensor $\Delta\mathbf{S}$ can be derived as $\Delta\mathbf{S} = \mathbb{C}_{\mathrm{ep}}\Delta\mathbf{E}$ with $\Delta\mathbf{E} := \frac{1}{2}(\Delta\mathbf{F}^{\mathrm{T}}\mathbf{F} + \mathbf{F}^{\mathrm{T}}\Delta\mathbf{F})$ and the consistent tangent matrix $\mathbb{C}_{\mathrm{ep}}$.

5. Numerical examples

The algorithmic formulation of the orthotropic constitutive model is implemented in an extended version of FEAP, a finite-element code documented in [13]. Two sets of simulations are conducted to test the behavior of the proposed orthotropic model as well as the robustness of the numerical methods. The simulations were run with an 8-node brick-type shell element using the ANS-method and a 5-parameter EAS concept (Q1A3E5), see [4].

5.1. Necking of a circular bar

The necking of a circular bar is an example widely investigated in the literature, see e.g. [14] or [4]. The geometrical data are $R = 6.413$ mm, $R_b = 0.982R$ and $L = 26.667$ mm. To initialize the necking process we use the reduced radius R_b at $z = 26.667$ mm as a geometrical imperfection. The material data for isotropic elasticity and the isotropic von Mises yield condition (24) with nonlinear isotropic hardening (25) are given as follows: $E = 206.9$ GPa, $\nu = 0.29$, $Y^0 = 0.45$ GPa, $Y^\infty = 0.715$ GPa, $\delta = 16.93$.

The finite element discretization of half the bar is depicted in Fig. 1. At $z = L$ we impose the symmetry boundary conditions $w = 0$ mm, whereas in a displacement controlled computation the axial elongation $w(z = 0\ \mathrm{mm})$ is prescribed. Furthermore, we consider symmetry conditions in the cross-section of the plane. Thus, one eighth of the entire bar of total length $2L$ is discretized with 960 elements. Fig. 2 displays the deformed structure at $w = 7$ mm and the equivalent plastic strain, which concentrate in the necking zone. The results are in very good agreement with the computational reference solutions in [4,14] (see Fig. 2). Before the onset of necking the result of our finite-element analysis is in accurate accordance with the experimental results reported in [15]; it captures pretty well the load bearing capacity of the bar of 79.2 kN, whereas for elongations $w > 4$ mm it is somewhat too weak.

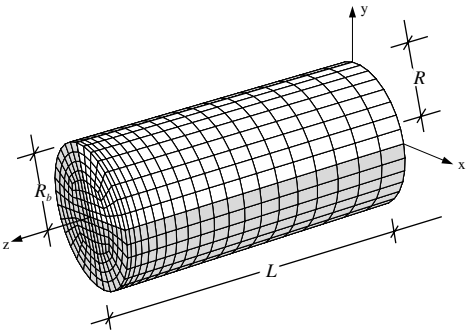

Fig. 1. Geometry and finite-element mesh.

5.2. Simply supported circular plate with uniform load

We now consider the elastoplastic deformation of a circular plate under dead load. The plate is simply supported in the z-direction at the bottom of the edges so that horizontal displacements and rotations at the edges may occur. Fig. 3 depicts the geometry of the problem and its finite-element discretization. With respect to symmetry only one quarter of the plate is discretized. The mesh is chosen with one element through the thickness and 192 elements in plane for each quadrant. The material is assumed to be isotropic in elasticity ($\mu = 80.19$ GPa and $\lambda = 110.74$ GPa) but orthotropic in its yield properties. The x- and y-axes of the coordinate system in Fig. 3 coincide with the axes of orthotropy. Two different materials are considered for orthotropic yielding. For material A the shear stresses dominate in the yield criterion,

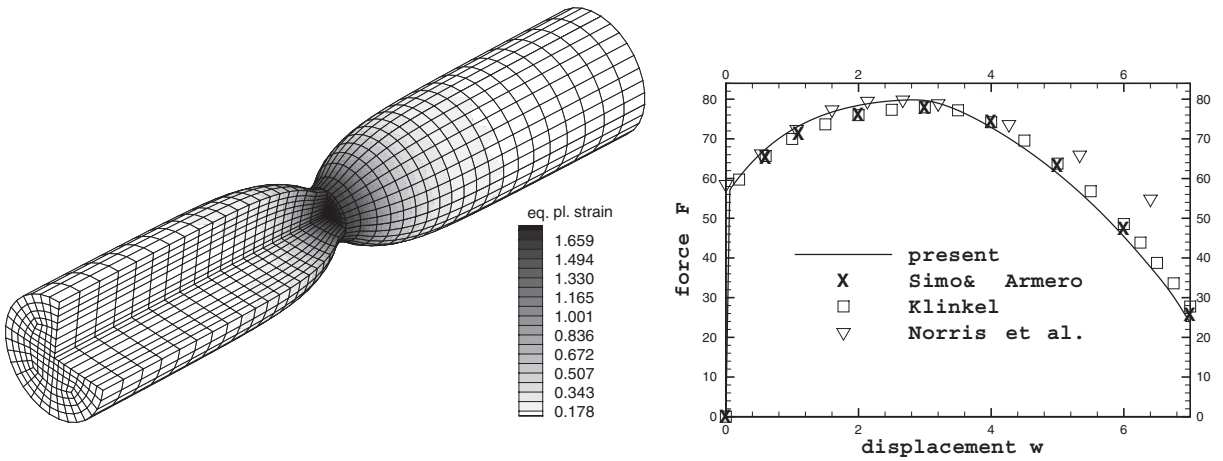

Fig. 2. Left: Equivalent plastic strain at $w = 7$ mm. Right: Computational and experimental results of applied force F [kN] versus axial elongation w [mm].

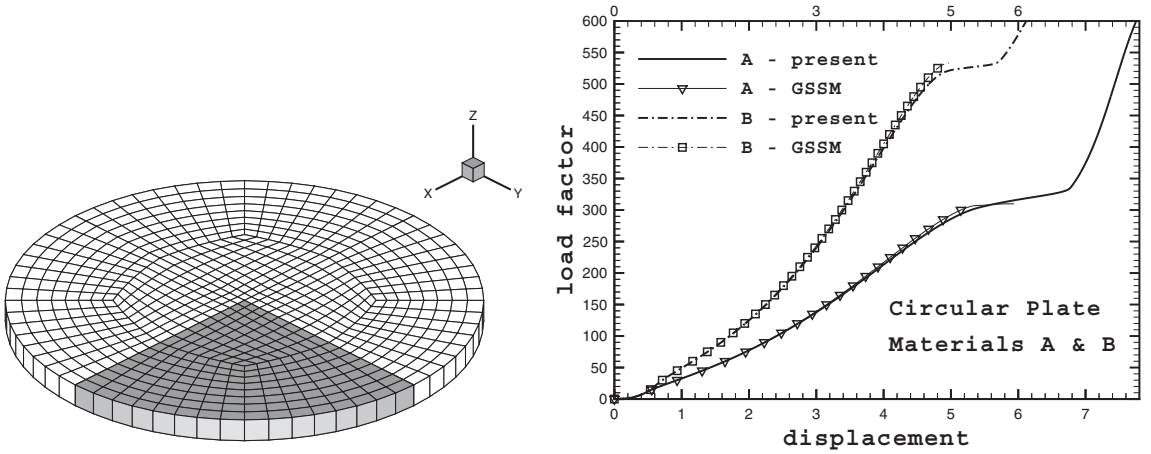

Fig. 3. Circular plate. Left: Geometry and finite-element mesh. Right: Load displacement curves for materials A and B. Multiplicative model (present) versus generalized stress strain measures for $m = 0$ (GSSM).

we set $Y_{xy} = 0.5 \cdot Y_{xx}/\sqrt{3}$. In contrast to A, for material B the normal stresses are predominant in yielding: for the shear yield stress we choose $Y_{xy} = 2.0 \cdot Y_{xx}/\sqrt{3}$ which is twice the isotropic value. For both materials $Y_{xx} = Y_{yy} = 0.45$ GPa holds.

Fig. 3 (right) depicts the load deflection curves where the load factor $\bar{\lambda}$ in $p_z(\bar{\lambda}) = \bar{\lambda} p_{z0}$ is plotted as a function of the vertical displacement of the center point of the circular plate. Remarkably, the results of the proposed multiplicative model and those obtained by a theory based on generalized stress–strain measures for parameter $m = 0$, which leads to logarithmic strains and conjugate stresses, are in very good agreement. For details of the latter formulation, we refer to [16]. The deflection of the plate at the load levels $\bar{\lambda} = 400$ for material A and $\bar{\lambda} = 600$ for material B is shown in Fig. 4. As expected the plastic strains concentrate for material A at a 45° angle in the (x, y)-plane and for material B along the x- and y-axes. Our finite-

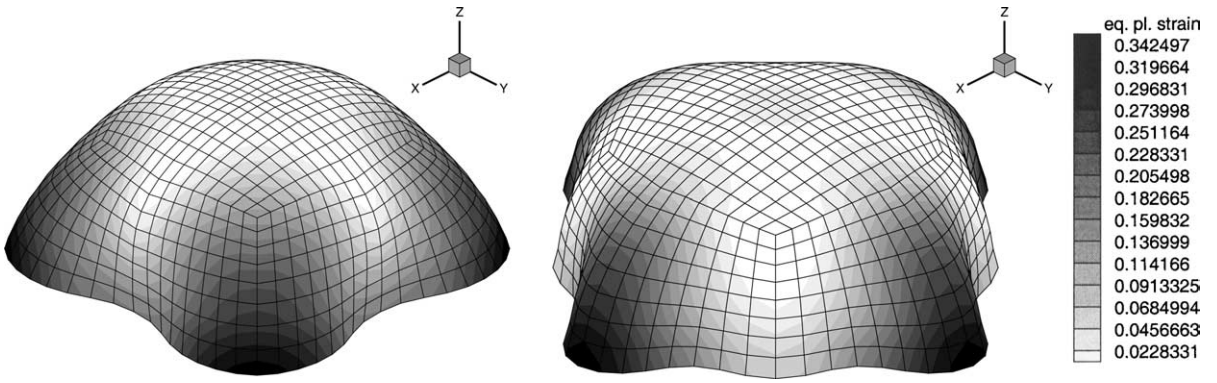

Fig. 4. Equivalent plastic strain on deformed structures from perspective view for material A at $\bar{\lambda} = 400$ (left) and for material B at $\bar{\lambda} = 600$ (right).

element simulation renders physically reasonable results concerning loci and number of the ears.

6. Conclusions

In this paper a multiplicative formulation of orthotropic elastoplasticity at finite inelastic strains is presented and aspects of its finite-element implementation are addressed. The governing constitutive equations, formulated in an invariant setting by the introduction of structural tensors, are formulated relative to the intermediate configuration. A quadratic yield function is expressed in terms of the symmetric part of the Mandel stresses. A general return algorithm along with an exponential map is applied, the latter fulfills plastic incompressibility exactly. In a representative numerical example we demonstrate the predictive capacity of our finite-element simulations to capture anisotropic phenomena such as '*earing*' closely related to deep-drawing processes of sheet metals.

Acknowledgements

Financial support for this research was provided by the Deutsche Forschungsgemeinschaft within SFB 298 TP A15, which is gratefully acknowledged.

References

[1] J. Betten, Formulation of anisotropic constitutive equations, in: J.P. Boehler (Ed.), Applications of Tensor Functions in Solid Mechanics, CISM Course no. 292, Springer, Heidelberg, 1987, pp. 227–250.
[2] J.P. Boehler, Introduction to the invariant formulation of anisotropic constitutive equations, in: J.P. Boehler (Ed.), Applications of Tensor Functions in Solid Mechanics, CISM Course no. 292, Springer, Heidelberg, 1987, pp. 13–30.
[3] A.J.M. Spencer, Theory of invariants, in: A.C. Eringen (Ed.), Continuum Physics, vol. 1, Academic Press, New York, 1971, pp. 239–353.
[4] S. Klinkel, Theorie und Numerik eines Volumen-Schalen-Elementes bei finiten elastischen und plastischen Verzerrungen, Ph.D. Thesis, Universität Karlsruhe (TH), 2000.
[5] J. Lubliner, Plasticity Theory, first ed., Macmillan Publishing Company, New York, 1990.
[6] J. Casey, P. Naghdi, A remark on the use of the decomposition $\mathbf{F} = \mathbf{F}_e\mathbf{F}_p$ in plasticity, J. Appl. Mech. 47 (1980) 672–675.
[7] J. Casey, P. Naghdi, A correct definition of elastic and plastic deformation and its computational significance, J. Appl. Mech. 48 (1981) 983–985.
[8] A.E. Green, P.M. Naghdi, Some remarks on elastic–plastic deformations at finite strains, Int. J. Eng. Sci. 9 (1971) 1219–1229.
[9] C. Miehe, E. Stein, A canonical model of multiplicative elasto-plasticity: formulation and aspects of the numerical implementation, Eur. J. Mech. A: Solids 11 (1992) 25–43.
[10] J.C. Simó, Algorithms for static and dynamic multiplicative plasticity that preserve the classical return mapping schemes of the infinitesimal theory, Comput. Methods Appl. Mech. Eng. 99 (1992) 61–112.
[11] C. Miehe, Exponential map algorithm for stress updates in anisotropic multiplicative elastoplasticity for single crystals, Int. J. Numer. Methods Eng. 39 (1996) 3367–3390.

[12] C. Sansour, F.G. Kollmann, Large viscoplastic deformations of shells. Theory and finite element formulation, Comput. Mech. 21 (1998) 512–525.
[13] R.L. Taylor, FEAP—A Finite Element Analysis Program: Users Manual, University of California, Berkeley, 2000. Available from <http://www.ce.berkeley.edu/rlt>.
[14] J.C. Simó, F. Armero, Geometrically non-linear enhanced strain mixed methods and the method of incompatible modes, Int. J. Numer. Methods Eng. 33 (1992) 1413–1449.
[15] D.M. Norris, B. Moran, J.K. Scudder, D.F. Quiñones, A computer simulation of the tension test, J. Mech. Phys. Solids 26 (1978) 1–19.
[16] J. Schröder, F. Gruttmann, J. Löblein, A simple orthotropic finite elasto-plasticity model based on generalized stress–strain measures, Comput. Mech. 30 (2002) 38–64.